Repetitive Penrose Process in Accelerating Kerr Black Holes

Xiao-Xiong Zeng[1,*] and Ke Wang[†2]

[1]*College of Physics and Electronic Engineering, Chongqing Normal University,*
Chongqing 401331, China

[2]*School of Material Science and Engineering, Chongqing Jiaotong University,*
Chongqing 400074, China

This paper investigates the repetitive Penrose process in accelerating Kerr black holes and explores the influence of the acceleration factor on the repetitive Penrose process. After a brief review of accelerating Kerr black holes, we study the fundamental equations of the Penrose process in this spacetime, examine the stopping conditions required for the repetitive Penrose process, and obtain corresponding numerical results. The conclusions indicate that, apart from the third law of thermodynamics similar to previous cases, accelerating Kerr black holes exhibit stronger energy extraction capabilities compared to Kerr black holes during the repetitive Penrose process. Moreover, in prior studies, the energy utilization efficiency was difficult to exceed 50%. However, in accelerating Kerr black holes, when the decay radius is relatively small, the energy utilization efficiency can exceed 50%, indicating that the reduced extractable energy primarily transforms into extracted energy rather than irreducible mass. On the other hand, when the initial value of the acceleration factor is large, the extractable energy can decrease to nearly zero, which also differs from the case of Kerr black holes in previous studies.

[†] Electronic address: kkwwang2025@163.com (Corresponding author)
[*]Electronic address: xxzengphysics@163.com

I. INTRODUCTION

The Penrose process is a mechanism for extracting energy from a rotating black hole [1]. In this process, a particle falls from infinity and decays within the ergosphere. One of the resulting particles carries negative energy and ultimately falls into the event horizon. Due to energy conservation, the other particle escapes to infinity carrying more energy than the original particle, which is equivalent to extracting rotational energy from the black hole. Since its proposal, this process has garnered widespread attention from physicists [2–10]. Research indicates that for energy extraction to be feasible, the velocity of the outgoing particle should exceed half the speed of light [11, 12].

Penrose's pioneering work has inspired physicists to explore various alternative mechanisms for extracting energy from black holes [13–22]. Recently, Ruffini et al. [23] achieved energy extraction by imposing a turning point condition on the particle's trajectory within the original equations of motion for the Penrose process in Kerr black holes. Furthermore, they proposed a repetitive Penrose process [24] (for related early work, see [25]). Research found that in the repetitive Penrose process, it is impossible to extract all the extractable energy from a Kerr black hole, the change in extractable energy primarily transforms into irreducible mass. This is because after each Penrose process, the new black hole mass and spin must be used for subsequent energy extraction, while also accounting for the new irreducible mass. The repetitive Penrose process is nonlinear, and the irreducible mass increases nonlinearly as well. The repetitive Penrose process proposed by Ruffini has since been extended to the repetitive electric Penrose process [26] and to Kerr-de Sitter black holes [27]. In the repetitive electric Penrose process, similarly, the total electric energy of a Reissner-Nordström black hole cannot be fully depleted, indicating that the repetitive Penrose process follows a pattern analogous to the third law of thermodynamics. In Kerr-de Sitter black holes, besides exhibiting phenomena similar to previous cases, the energy extraction capability in certain scenarios is stronger than that of Kerr black holes.

The C-metric is a special class of black hole solutions in general relativity, which can describe accelerating black holes [28] and belongs to the well-known Plebański–Demiański spacetime [29]. Accelerating black holes typically refer to black holes moving with acceleration along a certain direction under specific conditions, such as being influenced by extreme gravitational sources like cosmic strings. The inclusion of an acceleration factor fundamentally alters the causal structure and asymptotic properties of the black hole spacetime. Currently, many properties of accelerating black holes have been extensively studied [30–34]. In this paper, we aim to further investigate the repetitive Penrose process in accelerating Kerr black holes and explore the influence of the acceler-

ation factor on this process. In particular, we conduct a detailed study of several iterative stopping conditions. The results indicate that, apart from exhibiting a thermodynamic third law similar to previous cases, accelerating Kerr black holes possess stronger energy extraction capabilities compared to Kerr black holes during the repetitive Penrose process. Moreover, in prior research, the energy utilization efficiency was difficult to exceed 50%. However, in accelerating Kerr black holes, when the decay radius is relatively low, the energy utilization efficiency can exceed 50%, indicating that the reduced extractable energy primarily transforms into extracted energy rather than irreducible mass. On the other hand, when the initial value of the acceleration factor is large, the extractable energy can decrease to nearly zero, which also differs from previous conclusions. These findings demonstrate that conducting the repetitive Penrose process in accelerating Kerr black holes is easier and yields more extracted energy.

The remainder of this paper is organized as follows. In Section 2, we will introduce the Penrose process in accelerating Kerr black holes. In Section 3, we present the iterative stopping conditions for this process. In Section 4, we will study the repetitive Penrose process in accelerating Kerr black holes, with a particular focus on exploring the influence of the acceleration factor on this process. We conclude in Section 5. Throughout the paper, we will adopt natural units ($c = G = 1$).

II. THE PENROSE PROCESS IN ACCELERATING KERR BLACK HOLES

In the Boyer-Lindquist coordinates, the metric for an accelerating Kerr black hole is given by [33, 34]

$$ds^2 = \frac{1}{H^2} \left[\frac{1}{\alpha^2 \Sigma} \left(-\Delta_r + a^2 \Delta_\theta \sin^2\theta \right) dt^2 + \frac{2a\sin^2\theta}{\alpha\Sigma} \left(\Delta_r - \Delta_\theta(r^2 + a^2) \right) dt d\phi \right.$$
$$\left. + \frac{\Sigma}{\Delta_r} dr^2 + \frac{\Sigma}{\Delta_\theta} d\theta^2 + \frac{\sin^2\theta}{\Sigma} \left(-a^2\Delta_r \sin^2\theta + \Delta_\theta(r^2 + a^2)^2 \right) d\phi^2 \right], \tag{1}$$

where

$$H = 1 + Ar\cos\theta, \Sigma = r^2 + a^2\cos^2\theta, \Delta_r = (1 - A^2 r^2)(r^2 - 2Mr + a^2),$$
$$\Delta_\theta = 1 + 2MA\cos\theta + A^2 a^2 \cos^2\theta, \alpha = \sqrt{\frac{1 - a^2 A^2}{1 + a^2 A^2}}. \tag{2}$$

Here, M is the black hole mass, a is the black hole spin, and A is the acceleration factor. If $A = 0$, the metric reduces to the Kerr metric.

The event horizon of the black hole is determined by $\Delta_r = 0$, i.e.,

$$r_A = \frac{1}{A}, r_\pm = M \pm \sqrt{M^2 - a^2}. \tag{3}$$

Among these, r_A is the acceleration horizon, while r_+ and r_- represent the event horizon and the Cauchy horizon, respectively. In general, we have $r_- \leq r_+ < r_A$. In this paper, to maximize energy extraction, we adopt a simplifying assumption by considering the repetitive Penrose process for an extremal accelerating Kerr black hole on the equatorial plane, where the initial black hole spin is $a = M$. This simplification has been widely employed in references [24, 27].

The boundary of the black hole's ergosphere is determined by $g_{tt} = 0$. On the equatorial plane, the solution to this equation is

$$
\begin{cases}
r_{E0} = 0, \\
r_{E-} = \dfrac{1}{3}\left(-\dfrac{\sqrt[3]{Q}}{A^2} + \dfrac{A^2(3a^2 - 4M^2) - 3}{\sqrt[3]{Q}} + 2M\right), \\
r_{EA} = \dfrac{1}{6}\left(\dfrac{(1 - i\sqrt{3})\sqrt[3]{Q}}{A^2} - \dfrac{(1 + i\sqrt{3})\left(A^2(3a^2 - 4M^2) - 3\right)}{\sqrt[3]{Q}} + 4M\right), \\
r_E = \dfrac{1}{6}\left(\dfrac{(1 + i\sqrt{3})\sqrt[3]{Q}}{A^2} - \dfrac{(1 - i\sqrt{3})\left(A^2(3a^2 - 4M^2) - 3\right)}{\sqrt[3]{Q}} + 4M\right),
\end{cases}
\tag{4}
$$

where

$$
\begin{cases}
Q = A^6(9a^2 M - 8M^3) + 3\sqrt{3}\sqrt{D} + 18A^4 M, \\
D = A^6\left((a^2 A^2 - 1)^3 + A^2 M^2(-a^4 A^4 + 20a^2 A^2 + 8) - 16A^4 M^4\right).
\end{cases}
\tag{5}
$$

Here, $r_{E-} < 0$ and is therefore discarded. r_E is the ergosphere boundary of the event horizon, whose value is greater than the event horizon, and r_{EA} is the ergosphere boundary of the acceleration horizon, whose value is less than the acceleration horizon. In this paper, we extract energy from the ergosphere of the event horizon. Typically, $r_E < r_{EA}$. When the acceleration factor increases to a certain value, r_E and r_{EA} become equal. Beyond this value, the ergosphere ceases to exist, making energy extraction impossible. For example, for an extremal black hole with $a = M$, the acceleration factor $\hat{A} = AM = \sqrt{\frac{5\sqrt{5}}{2} - \frac{11}{2}} = 0.30028$, at which point $r_E = r_{EA} = \frac{1}{2}(\sqrt{5} + 3)M = 2.61803M$. Here, a hat over a symbol denotes a dimensionless quantity.

The surface area of the black hole's event horizon is

$$
S = \int_0^\pi \int_0^{2\pi} \sqrt{g_{\theta\theta} g_{\phi\phi}} \, d\phi d\theta = \frac{4\pi(r_+^2 + a^2)}{1 - A^2 r_+^2}.
\tag{6}
$$

The irreducible mass of the black hole is [35]

$$
M_{irr} = \sqrt{\frac{S}{16\pi}} = \sqrt{\frac{r_+^2 + a^2}{4(1 - A^2 r_+^2)}}.
\tag{7}
$$

Thus, the extractable energy can be expressed as

$$E_{extractable} = M - M_{irr} = M - \sqrt{\frac{r_+^2 + a^2}{4(1 - A^2 r_+^2)}}. \tag{8}$$

This represents the theoretically maximum extractable energy that can be extracted from an accelerating Kerr black hole. For an extremal black hole, the irreducible mass and the extractable energy are

$$M_{irr,0} = \frac{M}{\sqrt{2(1 - A^2 M^2)}}, E_{extractable,0} = M - \frac{M}{\sqrt{2(1 - A^2 M^2)}}. \tag{9}$$

Therefore, as $\hat{A}$ increases, the maximum extractable energy decreases. In Fig. 1, we plot the maximum extractable energy and the location of the ergosphere boundary at the event horizon for an extremal black hole as functions of AM. It can be observed that as $\hat{A}$ increases, the ergosphere
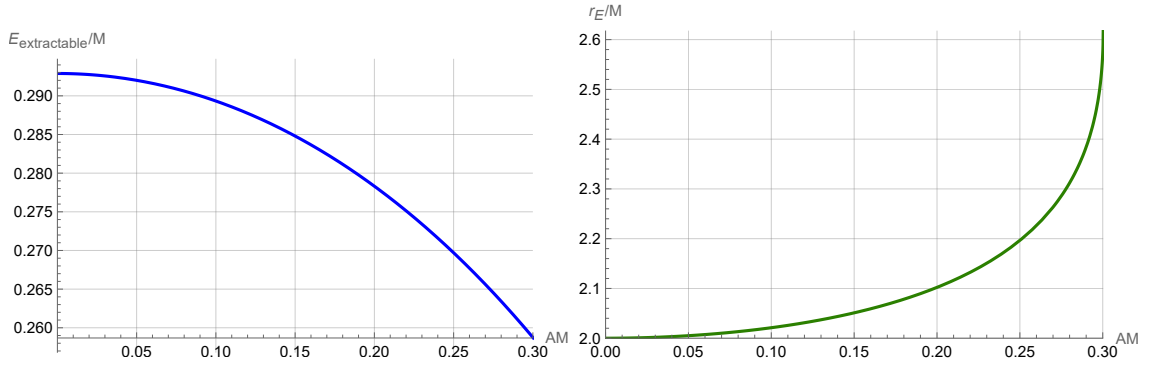

FIG. 1: Variation of $E_{extractable}/M$ and r_E/M with $\hat{A}$ for an extremal black hole.

boundary at the event horizon of the extremal black hole gradually increases, while the maximum extractable energy gradually decreases.

The fundamental equations of the Penrose process are given by 4-momentum conservation. The conservation equations for energy, angular momentum, and radial momentum can be expressed as

$$\begin{cases} \hat{E}_0 = \tilde{\mu}_1 \hat{E}_1 + \tilde{\mu}_2 \hat{E}_2, \\ \\ \hat{p}_{\phi 0} = \tilde{\mu}_1 \hat{p}_{\phi 1} + \tilde{\mu}_2 \hat{p}_{\phi 2}, \\ \\ \hat{p}_{r0} = \tilde{\mu}_1 \hat{p}_{r1} + \tilde{\mu}_2 \hat{p}_{r2}, \end{cases} \tag{10}$$

where

$$\hat{E}_i = E_i/\mu_i, \hat{p}_{\phi i} = p_{\phi i}/(\mu_i M), \hat{p}_{ri} = p_{ri}/\mu_i, \tilde{\mu}_i = \mu_i/\mu_0, i \in 0, 1, 2. \tag{11}$$

Here, μ_i is the mass of particle i. The effective potential for the radial motion of particles on the equatorial plane is given by [27]

$$\hat{V}_i^{\pm} = \frac{g^{t\phi}\hat{p}_{\phi i}M \mp \sqrt{(g^{t\phi})^2\hat{p}_{\phi i}^2 M^2 - g^{tt}(g^{\phi\phi}\hat{p}_{\phi i}^2 M^2 + 1)}}{g^{tt}}. \tag{12}$$

We focus on the optimal conditions for maximum energy extraction, where the radial momentum of all three particles must be zero at the decay position. This means that the three particles locates at their respective turning points, i.e., $\hat{E}_i = \hat{V}_i^+$. Specific reasons for this can be found in reference [27]. Under this condition, assuming $\hat{E}_0$, $\hat{p}_{\phi 1}$, and $\nu = \mu_2/\mu_1$ are known quantities, the fundamental equations of the Penrose process (10) have an analytical solution [27]

$$\begin{cases} \hat{p}_{\phi 0} &= \frac{g^{t\phi}\hat{E}_0 + \sqrt{(g^{t\phi})^2\hat{E}_0^2 - g^{\phi\phi}(1 + g^{tt}\hat{E}_0^2)}}{Mg^{\phi\phi}}, \\[2mm] \hat{E}_1 &= \frac{g^{t\phi}\hat{p}_{\phi 1}M - \sqrt{(g^{t\phi})^2\hat{p}_{\phi 1}^2 M^2 - g^{tt}(g^{\phi\phi}\hat{p}_{\phi 1}^2 M^2 + 1)}}{g^{tt}}, \\[2mm] \tilde{\mu}_1 &= \frac{\hat{E}_0\hat{E}_1 g^{tt} - \hat{E}_1 g^{t\phi}M\hat{p}_{\phi 0} - \hat{E}_0 g^{t\phi}M\hat{p}_{\phi 1} + g^{\phi\phi}M^2\hat{p}_{\phi 0}\hat{p}_{\phi 1} + \sqrt{F}}{\hat{E}_1^2 g^{tt} - 2\hat{E}_1 g^{t\phi}M\hat{p}_{\phi 1} + g^{\phi\phi}M^2\hat{p}_{\phi 1}^2 + \nu^2}, \\[2mm] \hat{E}_2 &= \frac{\hat{E}_0}{\tilde{\mu}_2} - \frac{\hat{E}_1}{\nu}, \hat{p}_{\phi 2} = \frac{\hat{p}_{\phi 0}}{\tilde{\mu}_2} - \frac{\hat{p}_{\phi 1}}{\nu}, \end{cases} \tag{13}$$

where

$$\begin{aligned} F = &- g^{tt}g^{\phi\phi}M^2\hat{E}_1^2\hat{p}_{\phi 0}^2 + (g^{t\phi})^2 M^2 \hat{E}_1^2 \hat{p}_{\phi 0}^2 - g^{tt}g^{\phi\phi}M^2\hat{E}_0^2\hat{p}_{\phi 1}^2 + (g^{t\phi})^2 M^2 \hat{E}_0^2 \hat{p}_{\phi 1}^2 \\ &+ 2g^{tt}g^{\phi\phi}M^2\hat{E}_0\hat{E}_1\hat{p}_{\phi 0}\hat{p}_{\phi 1} - 2(g^{t\phi})^2 M^2 \hat{E}_0\hat{E}_1\hat{p}_{\phi 0}\hat{p}_{\phi 1} - g^{tt}\hat{E}_0^2\nu^2 + 2g^{t\phi}M\hat{E}_0\hat{p}_{\phi 0}\nu^2 \\ &- g^{\phi\phi}M^2\hat{p}_{\phi 0}^2\nu^2. \end{aligned} \tag{14}$$

After each energy extraction, the remaining mass and angular momentum of the black hole are given by

$$M_n = M_{n-1} + \hat{E}_{1,n-1}\mu_{1,n-1}, L_n = L_{n-1} + \hat{p}_{\phi 1}\mu_{1,n-1}M_{n-1}, \tag{15}$$

where

$$L_0 = \hat{a}_0 M_0^2 = M_0^2. \tag{16}$$

This leads to corresponding changes in $\hat{a} = a/M$ and $\hat{A}$, namely

$$\Delta\hat{a}_{n-1} = \frac{L_n}{M_n^2} - \frac{L_{n-1}}{M_{n-1}^2}, \Delta\hat{A}_{n-1} = AM_n - AM_{n-1}. \tag{17}$$

The change in the event horizon is

$$\Delta r_{+,n-1} = M_n\left(1 + \sqrt{1 - \hat{a}_n^2}\right) - M_0\left(1 + \sqrt{1 - \hat{a}_0^2}\right). \tag{18}$$

The change in irreducible mass is

$$\Delta M_{irr,n-1} = \sqrt{\frac{r_{+,n}^2 + (\hat{a}_n M_n)^2}{4(1 - A^2 r_{+,n}^2)}} - \sqrt{\frac{r_{+,0}^2 + (\hat{a}_0 M_0)^2}{4(1 - A^2 r_{+,0}^2)}}. \tag{19}$$

The change in extractable energy is

$$\Delta E_{extractable,n-1} = \Delta M_{n-1} - \Delta M_{irr,n-1}. \tag{20}$$

During this process, the extracted energy is

$$E_{extracted,n} = M_0 - M_n. \tag{21}$$

The energy return on investment, defined as the ratio of extracted energy to the total energy of all incident particles from infinity, is given by [26]

$$\xi_n = E_{extracted,n}/(nE_0). \tag{22}$$

The energy utilization efficiency, defined as the ratio of extracted energy to the difference between the initial and final extractable energies, is given by [26]

$$\Xi_n = E_{extracted,n}/(E_{extractable,0} - E_{extractable,n}). \tag{23}$$

The above formulas will serve as important parameters for evaluating the strength of energy extraction and will be discussed in more detail later.

III.   ITERATIVE STOPPING CONDITIONS

During the repetitive energy extraction process, the aforementioned iteration cannot proceed indefinitely and must satisfy the following five conditions. First, the mass deficit must satisfy

$$1 - \tilde{\mu}_1 - \tilde{\mu}_2 > 0. \tag{24}$$

This condition is easily met if the parameters are appropriately chosen. Second, during the iteration, it is required that $\hat{E}_1 < 0$. Third, for each iteration, it must hold that $E_{extractable,n} > 0$. Fourth, for each iteration, the irreducible mass must not decrease. Since the irreducible mass remains constant under reversible transformations and increases under irreversible transformations, a decrease in irreducible mass is strictly prohibited, as this would correspond to a decrease in entropy. Finally, the turning points of particle 0 and particle 2 must lie to the right of the peak of their effective potentials, whereas the turning point of particle 1 must lie to the left of the peak of its effective

potential. The corresponding limiting case occurs when the classical turning point of each particle coincides exactly with the peak of its respective effective potential, i.e.,

$$\hat{V}_i^+(\hat{r}_d) = \hat{E}_i, \, d\hat{V}_i^+/d\hat{r}|_{\hat{r}=\hat{r}_d} = 0, \tag{25}$$

where $\hat{r}_d = r_d/M$ is the dimensionless decay radius. If $\hat{E}_0 = 1$, the lower spin limit for stopping the iteration is governed by particle 0, with its lower spin limit located at the corotating marginally bound orbit of that particle. The angular velocity for corotating Keplerian orbital motion in an accelerating Kerr black hole is given by [36]

$$\Omega_K = \frac{-\partial_r g_{t\phi} + \sqrt{(\partial_r g_{t\phi})^2 - (\partial_r g_{tt})(\partial_r g_{\phi\phi})}}{\partial_r g_{\phi\phi}} = \frac{\sqrt{M(1 + A^2 r^2) - A^2 r^3}}{\alpha \left(r^{3/2} + a\sqrt{M(1 + A^2 r^2) - A^2 r^3} \right)}. \tag{26}$$

The corresponding specific energy for corotating Keplerian orbital motion is [36]

$$\hat{\mathcal{E}} = -\frac{g_{tt} + g_{t\phi}\Omega_K}{\sqrt{-g_{tt} - 2g_{t\phi}\Omega_K - g_{\phi\phi}\Omega_K^2}} = \frac{(\Delta_r - a^2) + a\sqrt{r}X}{\alpha r\sqrt{\Delta_r - a^2 + 2a\sqrt{r}X - rX^2}}, \tag{27}$$

where

$$X = \sqrt{M(1 + A^2 r^2) - A^2 r^3}. \tag{28}$$

For a marginally bound orbit, $\hat{\mathcal{E}} = 1$. The lower spin limit for particle 0 can then be obtained by solving equation (27). If $\hat{E}_0 > 1$, the lower spin limit for stopping the iteration is governed by particle 2, with its lower spin limit located at the corotating photon sphere radius. The corotating photon sphere radius in an accelerating Kerr black hole satisfies [33]

$$(4r\Delta_r - \Sigma\partial_r\Delta_r)^2 = 16a^2 r^2 \Delta_r \Delta_\theta \sin^2\theta. \tag{29}$$

Thus, the lower spin limit for particle 2 can be obtained by solving equation (29). For the turning point of particle 1 to exist, the discriminant under the square root in the second formula of equation (13) must be positive, which corresponds to $\hat{r}_d$ being greater than the radius of the black hole's event horizon. The critical case occurs when $\hat{r}_d = \hat{r}_+$. Therefore, the lower spin limit for particle 1 is

$$\hat{a}_{min,1} = \sqrt{\hat{r}_d(2 - \hat{r}_d)}. \tag{30}$$

That is, the lower spin limit for particle 1 is independent of $\hat{A}$. In Fig. 2, we plot the variation of the lower spin limits for the three particles with $\hat{r}_d$ under different $\hat{A}$ values. For different $\hat{A}$ values, the ergosphere varies, leading to different allowable ranges for the decay radius. Furthermore, we
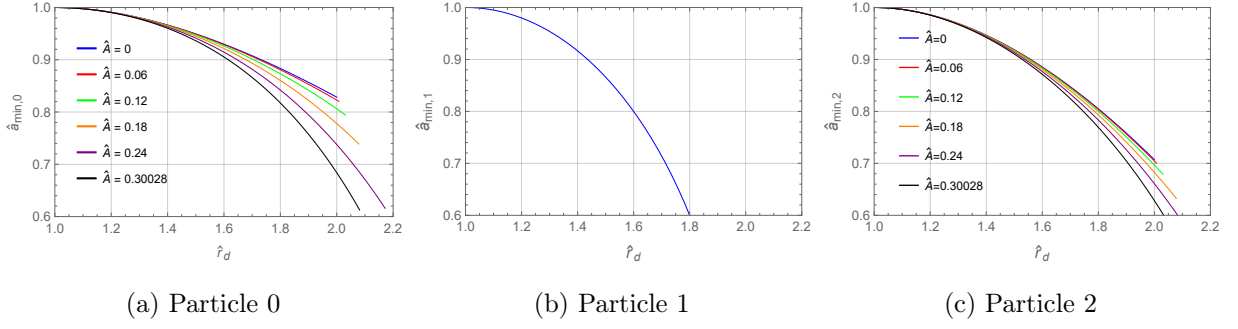
FIG. 2: Variation of the lower spin limit with decay radius $\hat{r}_d$ for different $\hat{A}$ values for (a) particle 0, (b) particle 1, and (c) particle 2.

have omitted the regions with large $\hat{r}_d$ and very small $\hat{a}_{min}$, which does not affect the overall trend. From Fig. 2, it can be observed that as the decay radius increases, the lower spin limits for all three particles decrease. As $\hat{A}$ increases, the lower spin limits for particle 0 and particle 2 decrease. This is a positive sign because a lower minimum spin indicates a greater number of possible iterations, thereby allowing more energy to be extracted during the repetitive Penrose process. Furthermore, unlike the Kerr-de Sitter spacetime where the lower spin limits for all three particles increase with the cosmological parameter $\hat{\Lambda}$ [27], the accelerating Kerr spacetime exhibits the opposite trend.

Next, in order to determine which of particles 0, 1, and 2 actually governs the lower spin limit for stopping the iteration, we plot Fig. 3. From the figure, it can be observed that $\hat{a}_{min,1} < \hat{a}_{min,2} <$
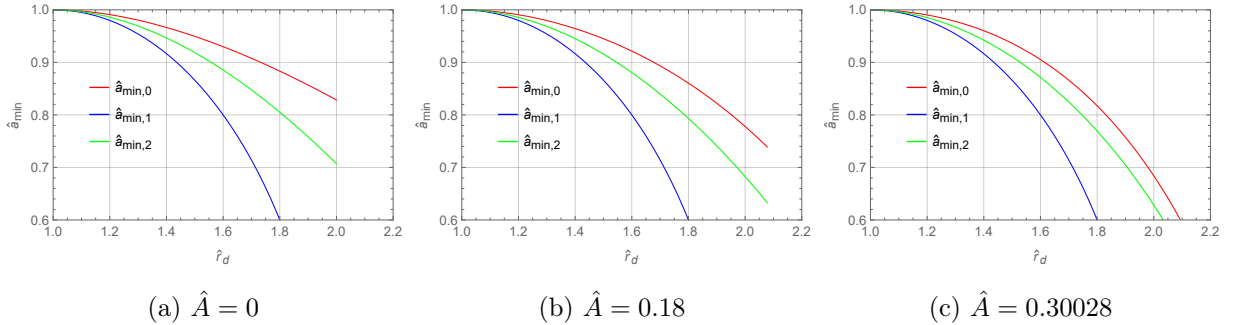
FIG. 3: Comparison of the lower spin limits for the three particles.

$\hat{a}_{min,0}$. Therefore, the lower spin limit for stopping the iteration is governed by particle 0. It is important to emphasize that this lower spin limit is not fixed. Because after each iteration, the mass M decreases, leading to a corresponding decrease in AM. Consequently, as inferred from Fig. 2a, the lower spin limit for stopping the iteration slightly increases with each iteration, but it will not exceed that of a Kerr black hole. The variation of the effective potential for particle 0 with $\hat{r}$

is plotted in Fig. 2 of Ref. [24], Fig. 6 of Ref. [27], and Fig. 2 of Ref. [26], further explaining why the lower spin limit for iteration stopping is controlled by particle 0.

IV.   REPETITIVE PENROSE PROCESS IN ACCELERATING KERR BLACK HOLES

In this section, we study the repetitive Penrose process. The results in reference [24] show that for cases with $\hat{E}_0 > 1$, the energy return on investment is lower than the case with $\hat{E}_0 = 1$. Therefore, we choose $\hat{E}_0 = 1$ to maximize the energy return on investment. Following reference [24], we set $\hat{p}_{\phi 1} = -19.434$, $\nu = \mu_2/\mu_1 = 0.78345$, and take $\mu_0 = 10^{-2}M$. We present the results in Table I. The initial dimensionless acceleration factor is taken as $\hat{A} = 0.3$, in which case the ergosphere is located at $\hat{r} \in (1, 2.5726)$. We choose the decay radius as $\hat{r}_d = 1.2$.

TABLE I: Repetitive Penrose process with initial $\hat{A} = 0.3$ and $\hat{r}_d = 1.2$.

n	$\frac{M_n}{M_0}$	$\hat{a}_n$	$\frac{\mu_{1,n}}{\mu_0}$	$\hat{E}_{1,n}$	$\frac{E_{extractable,n}}{M_0}$	$\frac{E_{extracted,n}}{M_0}$	$\frac{M_{irr,n}}{M_0}$	ξ_n	Ξ_n	$\hat{a}_{min,0,n}$
0	1.000000	1.000000	0.022251	-7.672332	0.258751	0.000000	0.741249	0.000000	0.000000	0.990248
1	0.998293	0.999084	0.022173	-7.691577	0.239495	0.001707	0.758798	0.170718	0.088659	0.990250
2	0.996587	0.998175	0.022093	-7.711233	0.231461	0.003413	0.765127	0.170630	0.125049	0.990253
3	0.994884	0.997274	0.022014	-7.731321	0.225307	0.005116	0.769577	0.170542	0.152982	0.990255
4	0.993182	0.996380	0.021933	-7.751866	0.220141	0.006818	0.773041	0.170455	0.176594	0.990257
5	0.991482	0.995493	0.021852	-7.772896	0.215616	0.008518	0.775866	0.170369	0.197484	0.990260
6	0.989783	0.994615	0.021770	-7.794440	0.211552	0.010217	0.778231	0.170283	0.216468	0.990262
7	0.988086	0.993745	0.021687	-7.816535	0.207844	0.011914	0.780243	0.170197	0.234030	0.990265
8	0.986391	0.992883	0.021604	-7.839220	0.204420	0.013609	0.781971	0.170112	0.250487	0.990267
9	0.984697	0.992030	0.021519	-7.862540	0.201234	0.015303	0.783463	0.170028	0.266055	0.990269
10	0.983006	0.991187	0.021433	-7.886547	0.198250	0.016995	0.784756	0.169945	0.280897	0.990272
11	0.981315	0.990352	0.021346	-7.911304	0.195441	0.018685	0.785875	0.169862	0.295131	0.990274

All data in Table I satisfy the iterative conditions. For example, according to the mass deficit formula (24), we obtain $\tilde{\mu}_1 < 1/(1 + \mu_2/\mu_1) = 0.56$. Additionally, for each iteration, the conditions $\hat{E}_1 < 0$ and $E_{extractable,n} > 0$ are also satisfied, and the irreducible mass does not decrease. The last column represents the lower spin limit for stopping the iteration after each step, indicating that this limit slightly increases with each iteration. At $n = 11$, the iteration has stopped. If we were to forcibly continue, we would have $\hat{a}_{12} = 0.989528$ and $\hat{a}_{min,0,12} = 0.990276$, which violates the iterative condition.

From Table I, it can be seen that a small portion of the reduction in extractable energy flows

into the extracted energy, while the majority flows into the irreducible mass. Based on the energy utilization efficiency, it is indicated that 29.5% of the change in extractable energy is converted into extracted energy, while 70.5% is converted into irreducible mass. The results show that reducing the black hole's spin cannot extract all the corresponding rotational energy. This limitation arises from the nonlinear increase in irreducible mass, which also demonstrates that the repetitive Penrose process follows a pattern analogous to the third law of thermodynamics. Furthermore, after the iteration terminates in the repetitive Penrose process, a remaining extractable energy of $0.195441M$ persists, indicating that a significant amount of energy remains to be extracted by other means. These results exhibit similarities with the case of Kerr black holes [24].

Next, we change the decay radius to $\hat{r}_d = 2.4$, keeping all other parameters the same as in Table I. The results are presented in Table II. From Table II, it can be observed that the iteration

TABLE II: Repetitive Penrose process with initial $\hat{A} = 0.3$ and $\hat{r}_d = 2.4$.

n	$\frac{M_n}{M_0}$	$\hat{a}_n$	$\frac{\mu_{1,n}}{\mu_0}$	$\hat{E}_{1,n}$	$\frac{E_{extractable,n}}{M_0}$	$\frac{E_{extracted,n}}{M_0}$	$\frac{M_{irr,n}}{M_0}$	ξ_n	Ξ_n	$\hat{a}_{min,0,n}$
0	1.000000	1.000000	0.027659	-0.077270	0.258751	0.000000	0.741249	0.000000	0.000000	0.166019
1	0.999979	0.994667	0.027516	-0.067348	0.212974	0.000021	0.787005	0.002137	0.000467	0.166052
2	0.999960	0.989356	0.027374	-0.057461	0.194108	0.000040	0.805852	0.001995	0.000617	0.166081
3	0.999944	0.984067	0.027233	-0.047609	0.179686	0.000056	0.820259	0.001854	0.000704	0.166105
4	0.999931	0.978800	0.027093	-0.037792	0.167569	0.000069	0.832363	0.001715	0.000752	0.166125
5	0.999921	0.973554	0.026954	-0.028009	0.156930	0.000079	0.842991	0.001577	0.000774	0.166141
6	0.999914	0.968330	0.026817	-0.018260	0.147344	0.000086	0.852569	0.001440	0.000775	0.166152
7	0.999909	0.963128	0.026680	-0.008545	0.138559	0.000091	0.861350	0.001304	0.000759	0.166160
8	0.999906	0.957947	0.026544	0.001138	0.130409	0.000094	0.869497	0.001170	0.000729	0.166163

terminates because $\hat{E}_{1,8} > 0$ during the 8th iteration, making the next iteration impossible.

Next, we change the decay radius to $\hat{r}_d = 2.2$, keeping all other parameters the same as in Table I. We present the results in Table III. According to Table III, the iteration stops at the 37th step. If we were to forcibly proceed to the 38th iteration, we would have $E_{extractable,38} = -0.002241 < 0$, which violates the iterative condition. From Table III, it can be seen that the irreducible mass reaches a remarkable $0.99679M$, leaving almost no remaining extractable energy. This indicates that under these parameters, nearly all of the extractable energy is converted into irreducible mass. The results shown in Table III differ from those of Kerr black holes, where, upon iteration termination, the remaining extractable energy is still relatively large, typically not less than $0.1M$ [24].

Finally, we change the decay radius to $\hat{r}_d = 1.06$, keeping all other parameters the same as

TABLE III: Repetitive Penrose process with initial $\hat{A} = 0.3$ and $\hat{r}_d = 2.2$.

n	$\frac{M_n}{M_0}$	$\hat{a}_n$	$\frac{\mu_{1,n}}{\mu_0}$	$\hat{E}_{1,n}$	$\frac{E_{extractable,n}}{M_0}$	$\frac{E_{extracted,n}}{M_0}$	$\frac{M_{irr,n}}{M_0}$	ξ_n	Ξ_n	$\hat{a}_{min,0,n}$
0	1.000000	1.000000	0.026873	-0.398875	0.258751	0.000000	0.741249	0.000000	0.000000	0.484488
1	0.999893	0.994991	0.026729	-0.390406	0.214372	0.000107	0.785521	0.010719	0.002415	0.484557
2	0.999788	0.990002	0.026587	-0.381968	0.196082	0.000212	0.803706	0.010577	0.003376	0.484624
3	0.999687	0.985034	0.026445	-0.373562	0.182102	0.000313	0.817585	0.010437	0.004085	0.484689
4	0.999588	0.980087	0.026304	-0.365186	0.170360	0.000412	0.829228	0.010297	0.004660	0.484753
5	0.999492	0.975161	0.026165	-0.356840	0.160053	0.000508	0.839439	0.010159	0.005146	0.484815
6	0.999399	0.970254	0.026026	-0.348525	0.150768	0.000601	0.848630	0.010022	0.005569	0.484875
7	0.999308	0.965369	0.025889	-0.340238	0.142262	0.000692	0.857046	0.009886	0.005941	0.484933
8	0.999220	0.960503	0.025753	-0.331981	0.134374	0.000780	0.864846	0.009751	0.006272	0.484990
9	0.999134	0.955658	0.025617	-0.323753	0.126992	0.000866	0.872142	0.009618	0.006570	0.485045
10	0.999051	0.950833	0.025483	-0.315553	0.120036	0.000949	0.879015	0.009485	0.006838	0.485098
11	0.998971	0.946028	0.025349	-0.307380	0.113445	0.001029	0.885526	0.009354	0.007081	0.485150
12	0.998893	0.941244	0.025217	-0.299236	0.107171	0.001107	0.891722	0.009224	0.007302	0.485200
13	0.998818	0.936479	0.025086	-0.291118	0.101177	0.001182	0.897641	0.009095	0.007503	0.485248
14	0.998745	0.931735	0.024955	-0.283028	0.095431	0.001255	0.903314	0.008967	0.007686	0.485295
15	0.998674	0.927010	0.024825	-0.274963	0.089908	0.001326	0.908766	0.008840	0.007853	0.485341
16	0.998606	0.922305	0.024697	-0.266925	0.084587	0.001394	0.914019	0.008714	0.008005	0.485384
17	0.998540	0.917620	0.024569	-0.258913	0.079450	0.001460	0.919090	0.008589	0.008144	0.485427
18	0.998476	0.912954	0.024443	-0.250927	0.074481	0.001524	0.923995	0.008465	0.008269	0.485468
19	0.998415	0.908308	0.024317	-0.242965	0.069668	0.001585	0.928747	0.008343	0.008383	0.485507
20	0.998356	0.903682	0.024192	-0.235028	0.064998	0.001644	0.933357	0.008221	0.008486	0.485545
21	0.998299	0.899075	0.024068	-0.227116	0.060463	0.001701	0.937836	0.008100	0.008579	0.485581
22	0.998244	0.894488	0.023945	-0.219228	0.056051	0.001756	0.942193	0.007980	0.008662	0.485616
23	0.998192	0.889920	0.023823	-0.211364	0.051757	0.001808	0.946435	0.007862	0.008736	0.485650
24	0.998141	0.885371	0.023701	-0.203523	0.047572	0.001859	0.950570	0.007744	0.008801	0.485682
25	0.998093	0.880842	0.023581	-0.195706	0.043490	0.001907	0.954604	0.007627	0.008858	0.485713
26	0.998047	0.876331	0.023461	-0.187911	0.039505	0.001953	0.958542	0.007511	0.008908	0.485743
27	0.998003	0.871840	0.023343	-0.180139	0.035613	0.001997	0.962390	0.007396	0.008950	0.485771
28	0.997961	0.867368	0.023225	-0.172390	0.031808	0.002039	0.966153	0.007282	0.008985	0.485798
29	0.997921	0.862914	0.023108	-0.164663	0.028085	0.002079	0.969835	0.007169	0.009014	0.485824
30	0.997883	0.858479	0.022992	-0.156957	0.024442	0.002117	0.973440	0.007057	0.009036	0.485848
31	0.997847	0.854064	0.022876	-0.149274	0.020875	0.002153	0.976972	0.006946	0.009052	0.485871
32	0.997813	0.849666	0.022762	-0.141611	0.017379	0.002187	0.980433	0.006836	0.009062	0.485893
33	0.997780	0.845288	0.022648	-0.133969	0.013953	0.002220	0.983828	0.006726	0.009067	0.485914
34	0.997750	0.840928	0.022535	-0.126349	0.010592	0.002250	0.987158	0.006618	0.009067	0.485933
35	0.997722	0.836586	0.022423	-0.118748	0.007295	0.002278	0.990427	0.006510	0.009061	0.485952
36	0.997695	0.832263	0.022312	-0.111168	0.004058	0.002305	0.993637	0.006403	0.009050	0.485969
37	0.997670	0.827958	0.022201	-0.103608	0.000881	0.002330	0.996790	0.006297	0.009035	0.485985

in Table I. We present the results in Table IV. From Table IV, it can be observed that the

TABLE IV: Repetitive Penrose process with initial $\hat{A} = 0.3$ and $\hat{r}_d = 1.06$.

n	$\frac{M_n}{M_0}$	$\hat{a}_n$	$\frac{\mu_{1,n}}{\mu_0}$	$\hat{E}_{1,n}$	$\frac{E_{extractable,n}}{M_0}$	$\frac{E_{extracted,n}}{M_0}$	$\frac{M_{irr,n}}{M_0}$	ξ_n	Ξ_n	$\hat{a}_{min,0,n}$
0	1.000000	1.000000	0.022403	-9.704367	0.258751	0.000000	0.741249	0.000000	0.000000	0.999111
1	0.997826	0.999990	0.022395	-9.701363	0.256326	0.002174	0.741500	0.217407	0.896561	0.999111

iteration stops after the first step. If we forcibly proceed to the second iteration, we find $\frac{M_{irr,2}}{M_0} = 0.740656 < \frac{M_{irr,1}}{M_0} = 0.741500$, meaning the irreducible mass decreases, which violates the iterative condition. Table IV reveals a remarkable phenomenon: the energy utilization efficiency reaches 89.6%. This indicates that under these parameters, the reduction in extractable energy is primarily converted into extracted energy rather than irreducible mass. This result is significantly different from previous findings [24, 26, 27], where the energy utilization efficiency rarely exceeded 50%. Furthermore, if the decay radius is too small, such as $\hat{r}_d = 1 - 1.05$, even a single iteration cannot satisfy the conditions, making energy extraction impossible because the irreducible mass becomes imaginary in such cases.

In Fig. 4, we plot the variation with decay radius $\hat{r}_d$ of the energy return on investment ξ, the energy utilization efficiency Ξ, the extracted energy $E_{extracted}/M_0$, the extractable energy $E_{extractable}/M_0$, and the irreducible mass $\frac{M_{irr}}{M_0}$ after the repetitive Penrose process terminates, under different initial $\hat{A}$ values.

From panels (a), (b), and (d) of Fig. 4, it can be observed that at the same decay radius, as the initial $\hat{A}$ increases, the values of the energy return on investment, the energy utilization efficiency, and the extracted energy almost all increase. An exception is a slight anomaly in the extracted energy for $\hat{A} = 0.30028$ at lower decay radii. This indicates that, in the repetitive Penrose process, accelerating Kerr black holes possess stronger energy extraction capabilities compared to Kerr black holes. From panel (c) of Fig. 4, it can be seen that at lower decay radii, the energy utilization efficiency of accelerating Kerr black holes can exceed 50%, suggesting that the reduced extractable energy is primarily converted into extracted energy rather than irreducible mass. This is a distinctive feature of accelerating Kerr black holes. From panel (e) of Fig. 4, it is evident that when the initial value of the acceleration factor is large, the extractable energy can decrease to nearly zero. However, in such cases, the extractable energy is mainly converted into irreducible mass rather than extracted energy, as reflected in panel (f) where, for example, the irreducible mass increases to almost 1. Overall, the extracted energy still constitutes only a small fraction of the
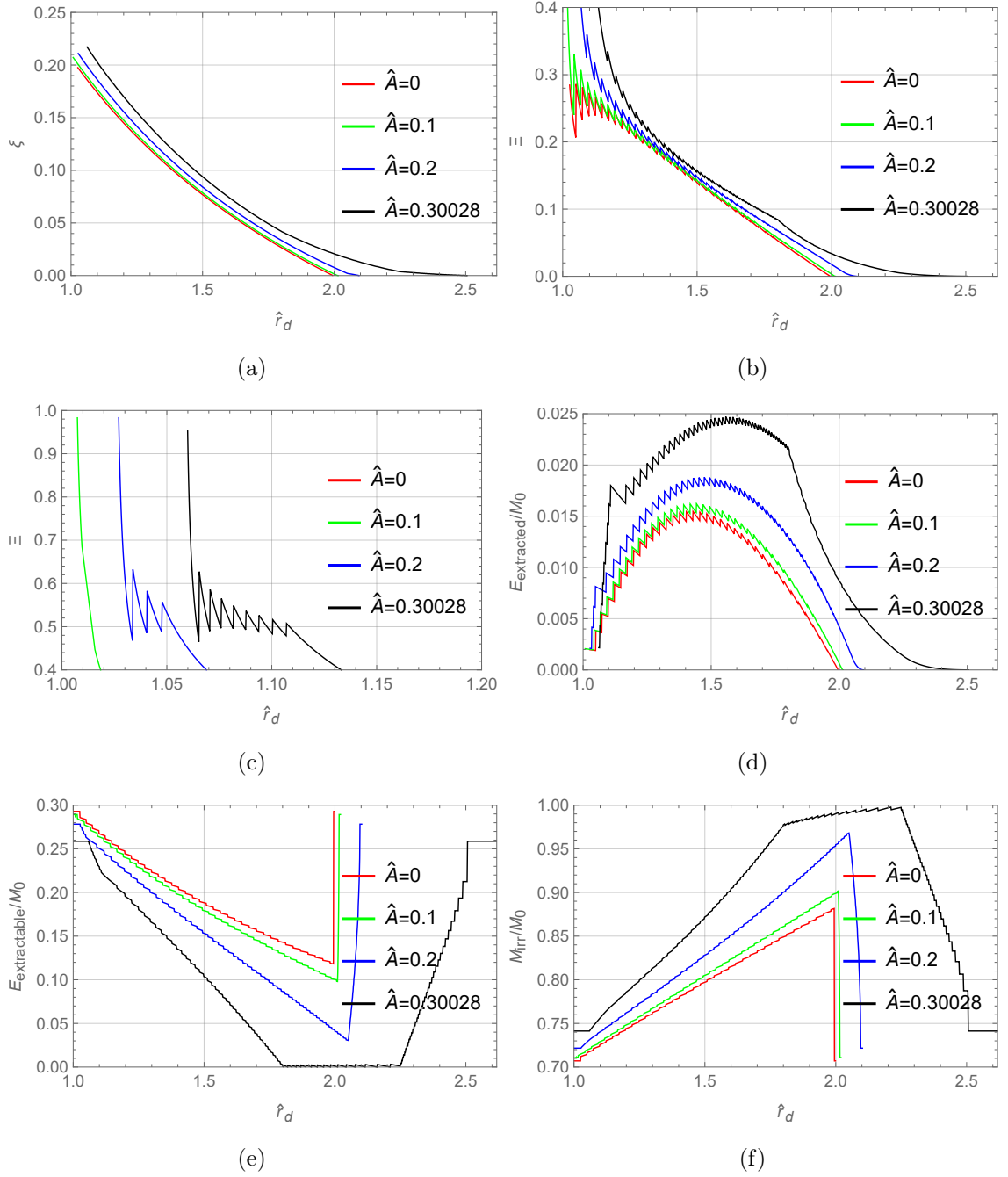
FIG. 4: Under different initial $\hat{A}$ values, after the termination of the repetitive Penrose process: (a) the energy return on investment ξ; (b, c) the energy utilization efficiency Ξ; (d) the extracted energy $E_{extracted}/M_0$; (e) the extractable energy $E_{extractable}/M_0$; (f) the irreducible mass $\frac{M_{irr}}{M_0}$ as functions of the decay radius $\hat{r}_d$. Each oscillation in the curves corresponds to a different number of iterations, caused by the iterative conditions and reflecting the discrete nature of the process.

initial black hole mass, not exceeding 2.5%. This shows that the repetitive Penrose process, even

when using the Ruffini process for energy extraction, still has significant limitations.

V. CONCLUSION

In this paper, under the optimal conditions for maximum energy extraction, we investigate energy extraction via the repetitive Penrose process in extremal accelerating Kerr black holes. First, we provide a brief review of accelerating Kerr black holes, including their horizons and ergospheres. Second, we introduce the fundamental equations of the Penrose process for accelerating Kerr black holes. Then, we describe the five iterative stopping conditions that the Penrose process must satisfy. In particular, we plot the variation of the lower spin limits for particles 0, 1, and 2 with the decay radius $\hat{r}_d$ under different $\hat{A}$ values, and compare the lower spin limits of the three particles, concluding that one of the lower spin limits for stopping the iteration is governed by particle 0. Finally, we present corresponding numerical results. Table I shows that the iteration stops due to the failure to meet the lower spin limit for particle 0; Table II shows that the iteration stops because $\hat{E}_1 > 0$; Table III shows that the iteration stops due to $E_{extractable} < 0$; and Table IV shows that the iteration stops because the irreducible mass begins to decrease.

Similar to previous conclusions, reducing the black hole's spin cannot extract all the corresponding rotational energy. This limitation arises from the nonlinear increase in irreducible mass, indicating that the repetitive Penrose process follows a pattern analogous to the third law of thermodynamics. The differences lie in the fact that, at the same decay radius, as the initial $\hat{A}$ increases, the values of the energy return on investment, the energy utilization efficiency, and the extracted energy almost all increase. This demonstrates that, in the repetitive Penrose process, accelerating Kerr black holes possess stronger energy extraction capabilities compared to Kerr black holes. When the decay radius is relatively low, the energy utilization efficiency of accelerating Kerr black holes can exceed 50%, indicating that the reduction in extractable energy is primarily converted into extracted energy rather than irreducible mass. Furthermore, when the initial value of the acceleration factor is large, the extractable energy can decrease to nearly zero. These phenomena are entirely different from those observed in Kerr black holes.

12375043, 12575069).

[1] R. Penrose, "Gravitational collapse: The role of general relativity," Riv. Nuovo Cim. **1** (1969), 252-276

[2] Z. Zhao, Z. Y. Fan, X. Wang, M. Guo and B. Chen, "Probing the Penrose Process: Images of Split Hotspots and Their Observational Signatures," [arXiv:2510.27409 [astro-ph.HE]].

[3] A. Kar, A. Dey and S. Kar, "A note on the Penrose process in rotating regular black holes," [arXiv:2510.11364 [gr-qc]].

[4] U. Fatima and G. Abbas, "Penrose Process Efficiency and Irreducible Mass in Rotating Einstein-Born-Infeld Black Holes with Nonlinear Electrodynamics," [arXiv:2509.19390 [gr-qc]].

[5] V. Vertogradov and A. Rincon, "Energy extraction and evolution of regular black holes: The case of Bardeen spacetime," Phys. Dark Univ. **50** (2025), 102066

[6] D. Ortiqboev, F. Atamurotov, A. Abdujabbarov, G. Mustafa and D. Amaro, "Oscillatory signature and mechanism of energy extraction around rotating black holes in the Einstein-Euler-Heisenberg theory," Phys. Rev. D **112** (2025) no.4, 044026

[7] K. Q. Abbasi, F. L. Carneiro and M. Z. A. Moughal, "Energy extraction from rotating black hole with quintessential energy through the Penrose process," Phys. Lett. B **867** (2025), 139592

[8] S. J. Zhang, "Penrose process in magnetized non-Kerr rotating spacetime with anomalous quadrupole moment," JCAP **12** (2025), 004

[9] T. Xamidov, M. Alloqulov and S. Shaymatov, "Electric Penrose process and collisions of particles near five-dimensional weakly charged Schwarzschild black hole," Eur. Phys. J. Plus **140** (2025) no.3, 182

[10] F. Camilloni and L. Rezzolla, "Self-consistent Multidimensional Penrose Process Driven by Magnetic Reconnection," Astrophys. J. Lett. **982** (2025) no.1, L31

[11] J. M. Bardeen, W. H. Press and S. A. Teukolsky, "Rotating black holes: Locally nonrotating frames, energy extraction, and scalar synchrotron radiation," Astrophys. J. **178** (1972), 347

[12] R. M. Wald, "Energy Limits on the Penrose Process," Astrophys. J. **191** (1974), 231

[13] S. V. Dhurandhar, "Energy-extraction processes from a kerr black hole immersed in a magnetic field. i. negative-energy states," Phys. Rev. D **29** (1984) no.12, 2712-2720

[14] S. V. Dhurandhar, "Energy-extraction processes from a kerr black hole immersed in a magnetic field. ii. the formalism," Phys. Rev. D **30** (1984) no.8, 1625-1631

[15] T. Piran, J. Shaham and J. Katz, "High efficiency of the penrose mechanism for particle collisions," Astrophys. J. Lett. **196** (1975), L107

[16] S. A. Teukolsky and W. H. Press, "Perturbations of a rotating black hole. III - Interaction of the hole with gravitational and electromagnetic radiation," Astrophys. J. **193** (1974), 443-461

[17] R. D. Blandford and R. L. Znajek, "Electromagnetic extractions of energy from Kerr black holes," Mon. Not. Roy. Astron. Soc. **179** (1977), 433-456

[18] M. Takahashi, S. Nitta, Y. Tatematsu and A. Tomimatsu, "Magnetohydrodynamic Flows in Kerr Geometry: Energy Extraction from Black Holes," Astrophys. J. **363** (1990), 206

[19] M. Banados, J. Silk and S. M. West, "Kerr Black Holes as Particle Accelerators to Arbitrarily High Energy," Phys. Rev. Lett. **103** (2009), 111102

[20] E. Battista, "Quantum Schwarzschild geometry in effective field theory models of gravity," Phys. Rev. D **109** (2024) no.2, 026004

[21] Z. L. Wang and E. Battista, "Dynamical features and shadows of quantum Schwarzschild black hole in effective field theories of gravity," Eur. Phys. J. C **85** (2025) no.3, 304

[22] L. Comisso and F. A. Asenjo, "Magnetic Reconnection as a Mechanism for Energy Extraction from Rotating Black Holes," Phys. Rev. D **103** (2021) no.2, 023014

[23] R. Ruffini, M. Prakapenia, H. Quevedo and S. Zhang, "Single versus the Repetitive Penrose Process in a Kerr Black Hole," Phys. Rev. Lett. **134** (2025) no.8, 081403

[24] R. Ruffini, C. L. Bianco, M. Prakapenia, H. Quevedo, J. A. Rueda and S. R. Zhang, "Role of the irreducible mass in repetitive Penrose energy extraction processes in a Kerr black hole," Phys. Rev. Res. **7** (2025) no.1, 013203

[25] C. W. Misner, K. S. Thorne, and J. A. Wheeler, Gravitation (W. H. Freeman, San Francisco, USA, 1973).

[26] L. Hu, R. G. Cai and S. J. Wang, "Third law of repetitive electric Penrose process," [arXiv:2510.26866 [gr-qc]].

[27] K. Wang and X. X. Zeng, "Repetitive Penrose process in Kerr-de Sitter black holes," [arXiv:2512.05491 [gr-qc]].

[28] J. B. Griffiths, P. Krtous and J. Podolsky, "Interpreting the C-metric," Class. Quant. Grav. **23** (2006), 6745-6766

[29] J. F. Plebanski and M. Demianski, "Rotating, charged, and uniformly accelerating mass in general relativity," Annals Phys. **98** (1976), 98-127

[30] M. Appels, R. Gregory and D. Kubiznak, "Thermodynamics of Accelerating Black Holes," Phys. Rev. Lett. **117** (2016) no.13, 131303

[31] K. Destounis, R. D. B. Fontana and F. C. Mena, "Stability of the Cauchy horizon in accelerating black-hole spacetimes," Phys. Rev. D **102** (2020) no.10, 104037

[32] K. Destounis, G. Mascher and K. D. Kokkotas, "Dynamical behavior of the C-metric: Charged scalar fields, quasinormal modes, and superradiance," Phys. Rev. D **105** (2022) no.12, 124058

[33] T. T. Sui, Q. M. Fu and W. D. Guo, "The shadows of accelerating Kerr-Newman black hole and constraints from M87*," Phys. Lett. B **845** (2023), 138135

[34] A. Anabalón, F. Gray, R. Gregory, D. Kubizňák and R. B. Mann, "Thermodynamics of Charged, Rotating, and Accelerating Black Holes," JHEP **04** (2019), 096

[35] D. Christodoulou and R. Ruffini, "Reversible transformations of a charged black hole," Phys. Rev. D **4** (1971), 3552-3555

[36] K. Wang and X. X. Zeng, "Energy extraction from the accelerating Kerr black hole via magnetic reconnection in the plunging region and circular orbit region," JCAP **11** (2025), 026